Indian Journal of Chemistry
Vol. 56A, November 2017, pp. 1111-1121

Catalytically active network-like gold nanostructures: Synthesis and study of growth mechanism

Md. Harunar Rashid

Department of Chemistry, Rajiv Gandhi University, Rono Hills, Doimukh 791 112, Arunachal Pradesh, India
Email: mhr.rgu@gmail.com

Received 17 May 2017; revised and accepted 23 October 2017

Generation of network-like Au nanostructures by the reduction of gold ions in aqueous solution by bismuth ammonium citrate at room temperature is reported. The as-synthesized Au nanostructures have been characterized by spectroscopic, microscopic and diffractometric techniques. Microscopic results confirm that variation of $HAuCl_4$ concentration in the reaction mixture results in the formation of different types of network-like Au nanostructures. Kinetic results indicate that these network-like Au nanostructures are formed by the oriented attachment based self-assembly of smaller sized spherical Au nanoparticles. X-ray diffraction studies reveal that the formed Au nanostructures are crystalline. These network-like Au nanostructures are catalytically active and can be used to catalyze both the reduction of *p*-nitrophenol and redox reaction between $K_3[Fe(CN)_6]$ and $Na_2S_2O_3$. Further, these network-like Au nanostructures are reusable in both types of reactions without much loss in their catalytic activity.

Keywords: Nanostructures, Self-assembly, Network-like nanostructures, Catalysts, Gold nanoparticles

Noble metal nanoparticles (NPs) with well-defined geometrical shapes exhibit optical[1, 2], electronic[3], and catalytic[4-6] properties that are not available in their size-selections especially with spherical particles. In the case of metals like gold (Au) NPs which have strong surface plasmon resonance (SPR) oscillation, this is particularly important as the shape selective Au NPs production gives an easy handle in tuning their properties like absorption and emission spectra[7], surface enhanced Raman spectra (SERS)[8, 9] and other nonlinear properties. Indeed several protocols have recently been developed for the generation of Au NPs over a wide range of chemical compositions, sizes and shapes[8-12], the results are still pouring in especially with respect to application oriented metallic particle generation. This is where further development is required and thus any improvement in the process or yield would be welcome.

Among the various synthetic methods, wet chemical approaches are gradually attracted the attention of the researchers in the field of materials science and nanotechnology. In this regard, there has been a steady progress in the synthesis of different shaped Au NPs using variety of reducing agents. But most of the wet chemical approaches require surfactant or polymeric template for controlling the size or shape of Au NPs. Among these surfactants or polymeric templates, most commonly used ones are alkylamines[8], poly(vinyl pyrrolidone) (PVP)[13, 14] and cetyltrimethyl ammonium bromide (CTAB)[15, 16]. Besides the use of such soft templates, hard templates are also used to tune the shape of Au NPs[17]. Additionally, externally added metal ions are sometimes used along with the surfactant additives to initiate the anisotropic growth in seed mediated growth of Au NPs[16]. In such methods, the soft templates used get adsorbed on a particular crystal plane and thereby modify the relative growth rate in different planes that ultimately results in the formation of anisotropic Au NPs. Although template-based methods can be used to tune the shape of Au NPs, there are disadvantages associated with such techniques. These include the removal of the templates after formation of Au NPs, which is necessary to harvest the resulting Au NPs and post synthesis etching to remove hard templates[17].

Compared to these template-based syntheses of anisotropic Au NPs, wet chemical approaches without any added template is limited. For example, Yi *et al.*[18] reported a facile method to synthesize flower-like Au nanostructures through a one-step reduction of $HAuCl_4$ with dopamine at room temperature. Sastry *et al.*[19] reported the synthesis of triangular Au NPs using plant extract as reducing-cum-shape directing agent. Recently, synthesis of different shaped Au NPs by *in situ* reduction technique using

different cationic citrate at room temperature was also reported[20, 21]. An amine containing organic ligand has been used to prepare shape-tunable Au NPs by Mandal and his group.[22] An *in situ* synthesis of tape-like Au NPs using environmentally benign bio-molecules at room temperature was reported by Mandal *et al*.[23] Therefore, the search for simple and effective kinds of wet chemical approaches under mild conditions is highly demanding for the synthesis of application oriented Au NPs.

In recent years, Au NPs have been widely used as catalysts in numerous important chemical transformations, including hydrogenation[24, 25], oxidation[26-28], reduction of nitrophenols[20, 21, 29-31], Suzuki and Heck type coupling[32-34]. To achieve a high performance-to-cost ratio, catalysts are required to have, amongst other important attributes, a large surface area of catalytically active metal. As such, metal NPs are, by virtue, highly suitable to serve as catalyst[35]. Moreover, catalysis with these systems often occurred at certain planes, which are much more prevalent in metal NP system[36]. Although, Au NPs has been used as catalyst in different organic reactions, but reduction of *p*-nitrophenol is the most widely studied system due to its simplicity in carry out the reaction and the toxicity of *p*-nitrophenol compounds.

In the present study, a simple template-less wet chemical route is reported to synthesize self-assembled network-like Au nanostructures from aqueous solution of $HAuCl_4$ via reduction using bismuth ammonium citrate as reducing agent. The effect of $[HAuCl_4]$/[citrate] ratio on size and morphology of Au nanostructures has also been investigated. Subsequently, the growth kinetics and the catalytic activity of these Au nanostructures towards borohydride reduction of *p*-nitrophenol and redox reaction between potassium ferricyanide and sodium thiosulfate have been investigated. The network-like Au nanostructures are recoverable and can be reused as catalyst for consecutive cycles of both the organic and inorganic reactions.

Materials and Methods

$HAuCl_4 \cdot 3H_2O$ (Aldrich), $K_3[Fe(CN)_6]$, *p*-nitrophenol, $NaBH_4$ and $Na_2S_2O_3$ (Merck, India) bismuth ammonium citrate (SRL, India), were used as received from the suppliers. All the solutions were prepared in triply distilled water. Glassware was cleaned using freshly prepared aqua-regia (1:3; HNO_3:HCl) and then rinsed thoroughly with doubly distilled water.

Synthesis of Au nanostructures using bismuth ammonium citrate

The Au nanostructures were synthesized by the reduction of $HAuCl_4$ with bismuth ammonium citrate (BAC) following the previously reported method with some modification[20]. In a typical synthesis, 0.140 mL of 0.01 M BAC solution was added to a mixture of 3.290 mL water and 0.07 mL of 0.01 *M* aqueous $HAuCl_4$ solution to get a $[HAuCl_4]$/[BAC] ratio (*R*) = 0.5. The reaction mixture was then kept undisturbed at room temperature for 5 h. This set of reaction and the resultant suspension was designated as sample BAC-Au-0.5 (see Table 1). Two similar sets of reactions were also carried out at $[HAuCl_4]$/[BAC] ratio of 1.0 and 1.75 (see Table 1 for reaction recipe). In these reactions, the concentration of BAC was kept constant and hence the variation of $[HAuCl_4]$/[BAC] ratio reflected the variation of the concentration of $HAuCl_4$ in the reaction medium.

Catalytic activity of network-like Au nanostructures

It is known that Au NPs are catalytically active for a variety of organic reactions. To check the catalytic activity of these Au nanostructures, the borohydride reduction of *p*-nitrophenol and redox reaction between $K_3[Fe(CN)_6]$ and $Na_2S_2O_3$ were chosen as model reactions. For this study, the solid Au nanostructures were isolated from the as-prepared colloidal suspension by centrifugation at 9500×g for 15 min. The isolated product was purified from any traces of unreacted metal ions and BAC by washing in two cycles with water and centrifugation and finally the products were dried in vacuum at 60 ºC for 12 h. These dried powders of Au nanostructures were then used as catalyst.

Borohydride reduction of p-nitrophenol

In a typical reaction, 0.10 mL of 0.3 *M* $NaBH_4$ solution was added to a stirring reaction mixture of 2.8 mL water, 0.1 mL of 0.003 *M* *p*-nitrophenol solution and 2.7 mg of purified and dried solid

Table 1 — Parameters for the preparation of Au nanostructures using bismuth ammonium citrate

Sample[a]	$[HAuCl_4]$ (*M*)	[BAC] (*M*)	*R* =$[HAuCl_4]$/ [BAC]	Yield (%)	Morphology[b]
BAC-Au-0.5	2.0×10^{-4}	4.0×10^{-4}	0.5	40	Network
BAC-Au-1.0	4.0×10^{-4}	4.0×10^{-4}	1.0	80	Network
BAC-Au-1.75	7.0×10^{-4}	4.0×10^{-4}	1.75	85	Network

[a]BAC-Au indicates bismuth ammonium citrate/$HAuCl_4$ system and the numerical values represent the molar ratio between $HAuCl_4$ and BAC.
[b]After 5 h reaction time.

network-like Au nanostructures (sample BAC-Au-0.5). The progress of the reaction was then monitored by recording the time-dependent UV-vis absorption spectra of the reaction mixture. Two more catalytic reactions were then performed with other samples of network-like Au nanostructures using same reaction recipe as mentioned above (see Table 2 for details).

Redox reaction between $K_3[Fe(CN)_6]$ and $Na_2S_2O_3$

In a representative catalytic redox reaction, 0.20 mL of 0.1 *M* $Na_2S_2O_3$ solution was added to a stirring mixture of 2.0 mL water, 0.20 mL of 0.01 *M* $K_3[Fe(CN)_6]$ solution and 1.0 mg of purified and dried solid network-like Au nanostructures (sample BAC-Au-0.5) at 25 ºC. The progress of the redox reaction was then monitored by recording the time-dependent UV-vis absorption spectra of the reaction mixture. Two more catalytic redox reaction of $K_3[Fe(CN)_6]$ with $Na_2S_2O_3$ were also performed using the same recipe as mentioned above but with different Au NPs samples (see Table 3 for details).

Reusability of network-like Au nanostructures

In the course of catalytic reaction with network-like Au NPs, it was noticed that the solid Au nanostructures are deposited within a short span of time if the stirring was stopped. Hence, the deposited Au nanostructures were collected from the reaction mixture of *p*-nitrophenol/ $NaBH_4$ system (sample BAC-Au-0.5) and $K_3[Fe(CN)_6]$/ $Na_2S_2O_3$ system (sample BAC-Au-1.0) by decantation of the suspension after first batch of each reactions. The isolated mass was then purified by two cycles of washing with water and finally the respective catalysis reactions were performed using such recovered Au nanostructures. This process was repeated for several cycles.

Characterization

Transmission electron microscopic studies of the as-prepared Au nanostructures were performed in a high-resolution JEOL electron microscope (model 2100EM) by casting a drop of each sample on a carbon coated copper grid. The excess solutions were soaked with a tissue paper followed by drying in air. The images were recorded at an accelerating voltage of 200 kV. Samples for X-ray diffraction studies were prepared by depositing the as-prepared colloidal suspensions on a microscopic glass slide followed by drying in air. The diffractogram was then recorded in a Seifert XRD 3000P diffractometer at an accelerating voltage of 35 kV using Cu k_α (λ = 1.54 Å) as X-ray source. UV-vis spectra of the as-prepared Au nanostructures were recorded in a Hewlett Packard 8453 diode-array spectrophotometer. The individual Au nanostructures suspensions were transferred to a quartz cuvette and the spectrum was recorded in the region of 400-1100 nm against water as the blank.

Table 2 — Catalytic data for borohydride reduction of *p*-nitrophenol by different Au nanostructures samples

Sample	Morphology	Amt (mg)	k_{app} (s^{-1})
BAC-Au-0.5	Network	2.7	6.7×10^{-3}
BAC-Au-1.0	Network	2.7	7.5×10^{-4}
BAC-Au-1.75	Network	3.0	8.2×10^{-4}

Table 3 — Catalytic data for redox reaction between $K_3[Fe(CN)_6]$ and $Na_2S_2O_3$ catalyzed by network-like Au nanostructures. [Reaction temp. = 25 ºC]

Sample	Morphology	Amt of Au NPs (mg)	k_{app} (s^{-1})
BAC-Au-0.5	Network	1.0	4.81×10^{-4}
BAC-Au-1.0	Network	1.7	6.99×10^{-4}
BAC-Au-1.75	Network	1.7	6.27×10^{-4}

For the catalytic studies, the aqueous mixture of either $K_3Fe(CN)_6$ or *p*-nitrophenol and solid network-like Au nanostructures was first taken in a quartz cuvette placed in the cell holder of the same spectrophotometer equipped with a temperature controller. To the stirred reaction mixture, was added $Na_2S_2O_3$ solution for $K_3Fe(CN)_6$ or $NaBH_4$ solution for *p*-nitrophenol and the time-dependent absorption spectra of the reaction mixture were recorded in kinetic mode operation.

Results and Discussion

When an aqueous solution of BAC was added to an aqueous $HAuCl_4$ solution, the yellow color of $AuCl_4^-$ ions gradually changes to colorless to bluish to purplish-red. This observation indicated the formation of Au NPs that was further confirmed by UV-vis spectroscopy. The morphological evolution of the formed Au NPs was then characterized by microscopic techniques.

Transmission electron microscopy (TEM)

A series of reactions was performed by adding a specified amount of BAC separately to varying amount of $HAuCl_4$ taken in labeled glass vials to achieve a desired *R*-values (e.g., 0.5, 1.0 and 1.75) (Table 1). Figure 1(a) shows the TEM images of sample BAC-Au-0.5 prepared at a molar ratio of $HAuCl_4$ to BAC, i.e., $[HAuCl_4]/[BAC] = 0.5$ (where $[HAuCl_4] = 2.0\times10^{-4}$ *M*). The image clearly demonstrated the formation of

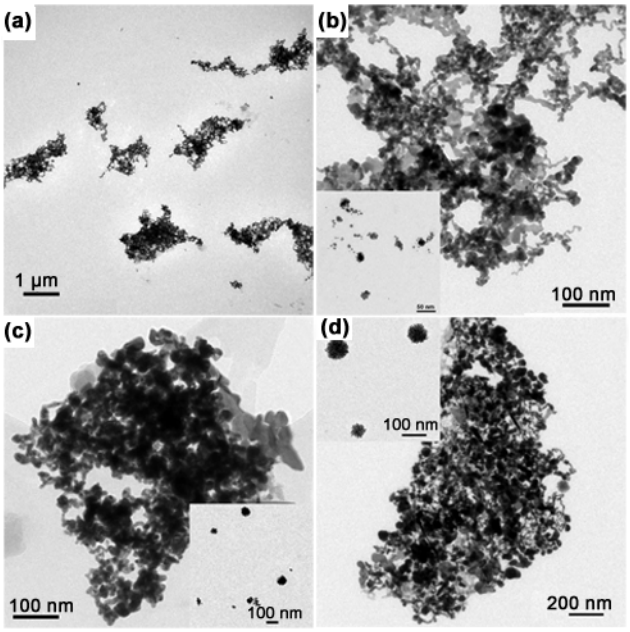

Fig. 1 — TEM images of Au nanostructures prepared at different [$HAuCl_4$]/[BAC] ratios: (a, b) BAC-Au-0.5, (c) BAC-Au-1.0, (d) BAC-Au-1.75. [The images were recorded after 5 h of reaction. Insets in panels 'b', 'c', and 'd' show TEM images of the respective samples recorded from different parts of the TEM grid].

network-like nanostructures after 5 h of reaction. High magnification TEM image of such network-like Au nanostructure as shown in Fig. 1(b) revealed that smaller sized Au NPs are fused together to form such nanostructures as no separation between the adjacent particles was observed. Additionally, some undeveloped assembled morphologies composed of spherical Au NPs were also observed in few places of the TEM grid (inset in Fig. 1(b)). This indicates that spherical Au NPs are formed at early stages of growth by fast nucleation, which was then assembled as the reaction proceeded to produce such network-like nanostructures. However, such isolated spherical particles could not be detected at early stages which may be due to the formation of Au NPs by fast nucleation as discussed below.

Previous reports suggest that variation of either the concentration of reducing agent or the concentration of metal precursor in the reaction medium results in the formation of different shaped or sized MNPs[21, 22, 37, 38]. So, in the present study, the metal ion concentration was varied keeping the concentration of citrate salt the same with the expectation that it will affect the size and shape of Au NPs. First of all, the concentration of $HAuCl_4$ was increased from 2.0×10^{-4} to 4.0×10^{-4} *M* in the reaction media to get the value of R = 1.0 (sample BAC-Au-1.0). The TEM image of sample BAC-Au-1.0 recorded after 5 h of reaction again shows the presence of network-like Au nanostructures (Fig. 1c). Similar to the earlier sample (sample BAC-Au-0.5), these nanostructures are also formed via the assembly of smaller sized Au NPs. However, these network-like Au nanostructures are quite different from those observed in the case of BAC-Au-0.5 prepared at [$HAuCl_4$]/[BAC] = 0.5. Besides the presence of network-like structures, the formation of spongy Au nanostructures was also noticed in some parts of the TEM grid (inset in Fig. 1C). This might indicate that spongy Au Nanostructures are the intermediate to these network-like Au nanostructures. Further increase in the concentration of $HAuCl_4$ to 7.0×10^{-4} *M* in sample BAC-Au-1.75 (prepared with [$HAuCl_4$]/[BAC] = 1.75) resulted in the formation of network-like morphologies as observed from the corresponding TEM image shown in Fig. 1(d). These network-like Au nanostructures are slightly different from those of the previous two samples (BAC-Au-0.5 and BAC-Au-1.0). Like sample BAC-Au-1.0, in this case also spongy Au nanostructures were observed in few places of the TEM grid (inset in Fig. 1d). On comparison of the TEM images in Fig. 1, one can easily visualize that as the concentration of $HAuCl_4$ is increased, the network-like structures are accompanied by some bigger particles in their backbone. This might be the fact that Au nanostructures prepared at lower [$HAuCl_4$]/[BAC] ratio resulted in the formation of more stable Au nanostructures due to relatively higher concentration of BAC that stabilizes the nanostructures more effectively than other samples prepared at higher concentration of $HAuCl_4$ and thereby preventing secondary growth. Further, the TEM results of samples BAC-Au-0.5, BAC-Au-1.0, and BAC-Au-1.75 (Fig. 1) revealed that that during the growth of Au nanostructures, smaller sized particles may be formed at the early stages by fast nucleation that gradually assembled as the reaction proceeded to form spongy and finally to network-like Au nanostructures. The details of mechanistic studies are discussed later in this section. The size and length of the network-like structure are not measurable because of their coiling nature (Fig. 1).

The energy dispersive X-ray (EDX) spectra recorded from sample BAC-Au-1.0 during TEM analysis showed the presence of intense peaks due to elemental gold along with a weak peak corresponding to Bi (Fig. 2). The signal of Cu is due to the use of Cu grid for preparing TEM sample. These results indicate

that the Bi^{3+} ions associated with BAC may be getting adsorbed on the surface of growing Au NPs during the reduction of Au^{3+} ions by citrate and thereby assisting the formation of such network-like Au nanostructures. Earlier, Sun *et al.*[39] have reported the formation of network-like Au nanostructures assisted by Ag^{+} ion during the reduction of $HAuCl_4$ by mercaptosuccinic acid.

X-ray diffraction

X-ray diffraction (XRD) studies were performed to investigate the crystalline nature of network-like Au nanostructures prepared using BAC. Figure 3 shows the XRD patterns of all the samples recorded after 5 h of reaction. The diffractograms are dominated by an intense diffraction peak at 2θ = 38.2°, corresponding to the (111) lattice plane of face centered cubic (fcc) Au (JCPDS card no. 4-0784). Besides this, weak intense peaks belonging to (200) lattice plane of fcc gold are also present at 2θ = 44.4º. However, other characteristic peaks due to (220) and (311) planes are almost absent in all the samples. These results clearly indicate the formation of well crystalline face centered cubic (fcc) gold bound by the (111) plane. Besides the representative peaks of the fcc gold, a relatively weak diffraction peak at 2θ = 41º was also observed in samples BAC-Au-1.75 and BAC-Au-1.0. This peak may be due to the presence of Bi related impurity in the sample that got adsorbed on the surface of growing Au NPs.

Spectrophotometry studies

The progress of the reaction between $HAuCl_4$ and BAC was monitored visually as well as via UV-vis spectroscopy. Figure 4 shows a set of UV-vis spectra of the as-prepared colloidal suspensions of Au prepared at different *R*-values (Table 1). All the absorption spectra recorded after 5 h show a rather similar nature and are dominated by a strong SPR absorption band in the region of 550-600 nm (Fig. 4(a–c)). For example, the colloidal Au NPs sample prepared at $[HAuCl_4]/[BAC] = 0.5$ shows the presence of a broad SPR band centered at 590 nm (Fig. 4a). As the concentration of $HAuCl_4$ was increased in the reaction medium, the peak become sharper with a blue shift in terms of peak position that ultimately appeared at 550 nm in case of sample BAC-Au-1.0 (Fig. 4b). A further increase in the concentration of $HAuCl_4$ results only in the increase in the intensity of the SPR band (Fig. 4c). These differences in absorbance and SPR band position might arise due to the differences in the size as well as

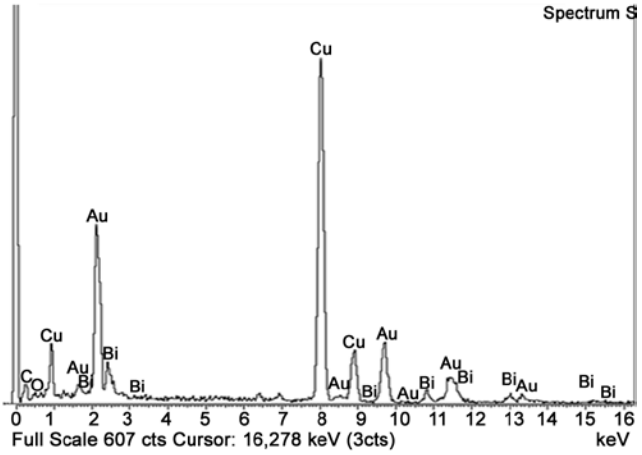

Fig. 2 — EDX spectra of Au nanostructures prepared using BAC (BAC-Au-1.0).

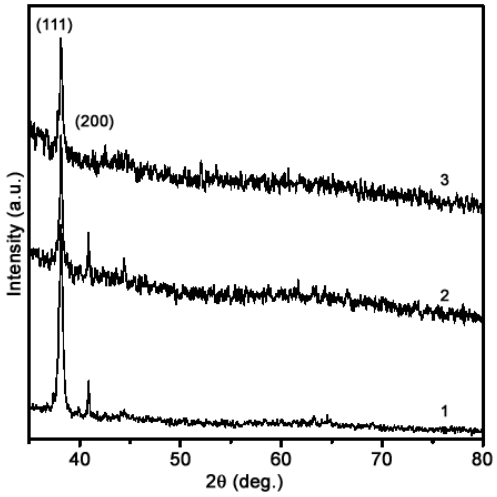

Fig. 3 — XRD patterns of Au nanostructures prepared at different *R* values: samples. [(1) BAC-Au-1.75; (2) BAC-Au-1.0; (3) BAC-Au-0.5].

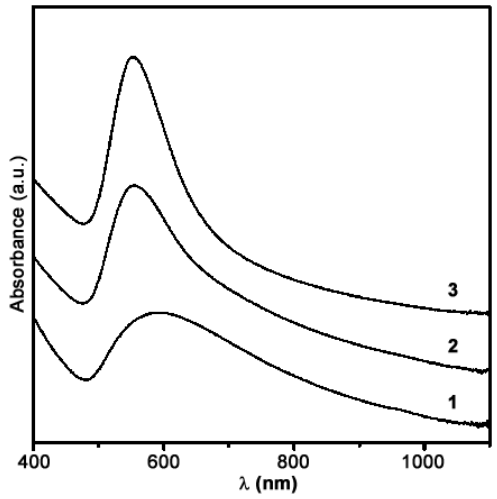

Fig. 4 — UV-vis spectra of the suspensions of different colloidal Au NPs recorded after 5 h of reaction. [(1) BAC-Au-0.5; (2) BAC-Au-1.0; (3) BAC-Au-1.75].

the branching of the nanostructures during its formation. However, these results are in good agreement with the UV-vis spectra of network-like Au nanostructures reported by other researchers[40].

Growth kinetics of network-like gold nanostructures formation

The growth kinetics of the formation of network-like Au nanostructures was studied by acquiring the time-dependent UV-vis spectra as well as the TEM analysis of sample BAC-Au-1.0 taken time to time during its formation. Figure 5 shows the typical time evolution of UV-vis spectra of colloidal Au NPs recorded during its formation. When aqueous solution of BAC was added to the reaction mixture, gradual fading of yellow color corresponding to $AuCl_4^-$ ions was observed. UV-vis spectra recorded after 6 and 11 min of reaction (see Fig. 5a and Fig. 5b) did not show any peak corresponding to Au NPs. As the reaction proceeded, the gradual development of pale-bluish color in the reaction medium was observed and the spectrum recorded after 14 min of reaction clearly showed a broad SPR band centered at 562 nm (Fig. 5c). The appearance of such broad band might indicate the formation of aggregated structures as reported earlier[41]. The corresponding TEM image shows the formation of assembled structures of Au NPs (Fig. 6a). Besides these nanostructures, some wire-like nanostructures as well as tiny spherical Au NPs (inset in Fig. 6A) were also observed in few places of the TEM grid. As the reaction proceeded, the SPR band gradually becomes sharper with a shifting in the blue region and the spectrum recorded after 25 min of reaction showed the maximum absorbance at 555 nm (Fig. 5e). The TEM image of the corresponding sample shows the formation of predominantly well-grown spongy Au nanostructures (Fig. 6b). The sizes of these Au nanostructures are in the ranges of 120-440 nm. As the reaction proceeded further, the peak position was further blue shifted to 550 nm after 50 min (Fig. 5g) and the corresponding TEM image again shows the presence of spongy Au nanostructures (Fig. 6c). However, in this case the sizes of these spongy Au nanostructures are observed to be smaller and varied between 100 and 325 nm. The absorption spectra recorded after 75 min of reaction shows the presence of SPR band at 543 nm (Fig. 5h) and the corresponding TEM image of this sample are dominated by spongy Au nanostructures of sizes ranging from 65–175 nm (Fig. 6d). These results clearly indicate that at the early stages (14 min), assembled nanostructures of Au are formed along

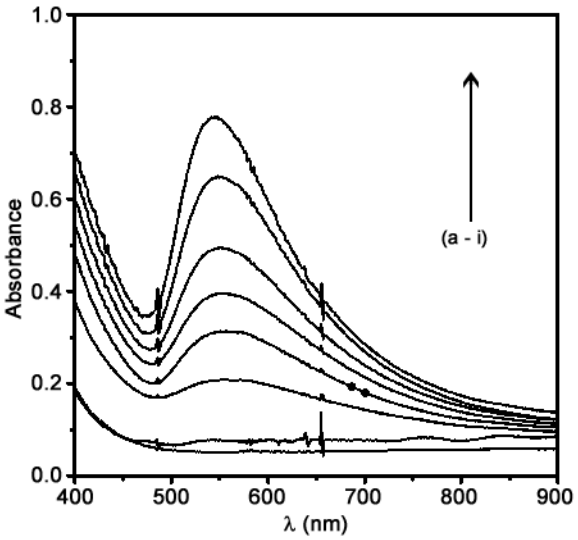

Fig. 5 — Time-evolution UV-vis spectra of the network-like Au nanostructure, BAC-Au-1.0, recorded during its formation. [(a) 6; (b) 11; (c) 14; (d) 20; (e) 25; (f) 33; (g) 50; (h) 75; (i) 180 min of reaction].

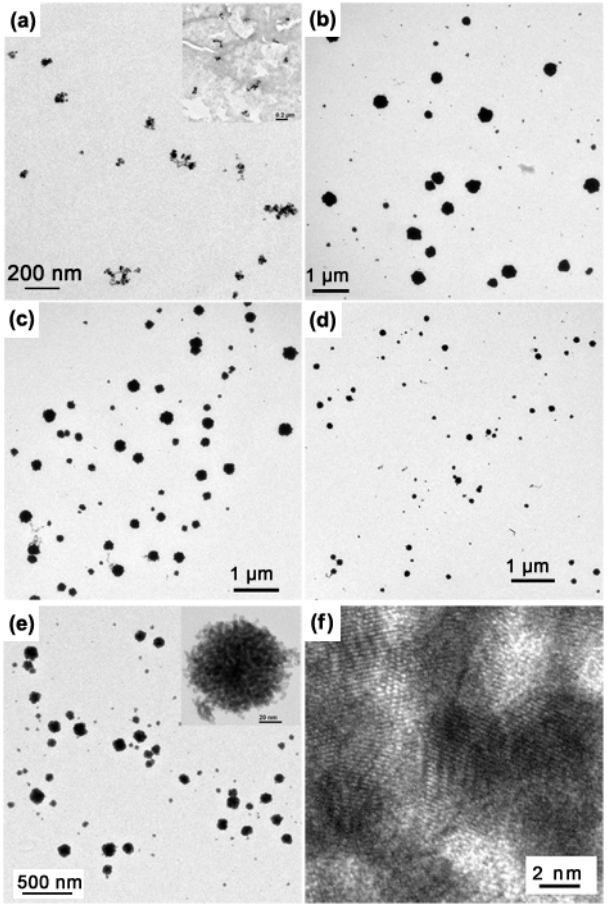

Fig. 6 — Time-dependent TEM images of BAC-reduced Au nanostructure of BAC-Au-1.0 recorded after varying reaction time (min). [(a) 14, (b) 25, (c) 50, (d) 75 and (e) 180 min]. (f) HRTEM image of a portion of spongy Au nanostructure shown in panel 'e'. [Inset in panel 'e' shows magnified TEM image of a spongy Au nanostructure].

with spherical NPs. As the reaction proceeded, the population of smaller sized spherical Au NPs increases, which eventually got assembled to form larger sized spongy Au nanostructures. After a certain time, say 25 min, these spongy Au nanostructures may undergo size reduction by the detachment of smaller Au NPs from the spongy structures to form smaller spongy nanostructures. This claim is supported by the UV-vis spectra where shifting of peak position in the blue region was observed and also further confirmed from the TEM image recorded after 50 min (Fig. 6c). The TEM image shown in Fig. 6c clearly shows the detachment of particles from spongy Au nanostructures. Finally, the SPR band appeared at 540 nm after 3 h of reaction (Fig. 5i). The TEM image recorded after 3 h shows the presence of spongy Au nanostructures of size ranges in between 35 to 160 nm (Fig. 6e). These TEM results match well with the results of UV-vis studies. A magnified TEM image of the spongy structure (inset in Fig. 6e) demonstrated that these spongy Au nanostructures are not a single particle; rather they are formed via the assembly of nearly monodispersed spherical Au NPs of average diameter of about 5 nm. This fact was further proved from the HRTEM image recorded from a portion of a spongy particle (Fig. 6f), which clearly showed the presence of well-resolved lattice fringes with an interplanar distance of 0.23 nm, corresponding to the (111) lattice plane of Au. This indicates the formation of well crystalline Au nanostructures that self-assembled orientally along the (111) direction to form spongy Au nanostructures. However, these spongy Au nanostructures are not stable enough and hence, on aging some portion of these structures detach resulting in the formation of smaller-sized branched network-like structures as evidenced from the TEM image recorded after 5 h of reaction (Fig. 1c).

Borohydride reduction of *p*-nitrophenol catalyzed by network-like Au nanostructures

It was observed that aqueous solution of *p*-nitrophenol shows absorption at 317 nm that was red shifted to 400 nm after addition of $NaBH_4$ (alkaline condition) due to the formation of *p*-nitrophenolate ion. In the absence of a catalyst, this absorption band remains unaltered with time, indicating that no conversion is taking place in the absence of a catalyst. However addition of a small amount of Au nanostructures (Table 2) to the reaction mixture causes fading and ultimate bleaching of the yellow color of the reaction mixture in quick succession. These changes were monitored by recording the time dependent UV-vis spectra of this catalytic reaction mixture. Figure 7(a) shows a typical time evolution UV-vis spectra of *p*-nitrophenol during its reduction in presence of network-like Au nanostructures (sample BAC-Au-0.5) that clearly show the disappearance of the peak at 400 nm corresponding to *p*-nitrophenolate ions with time. Subsequently, a gradual development of a new peak at 300 nm corresponding to *p*-aminophenol was observed (Fig. 7a). The spectroscopic results indicate

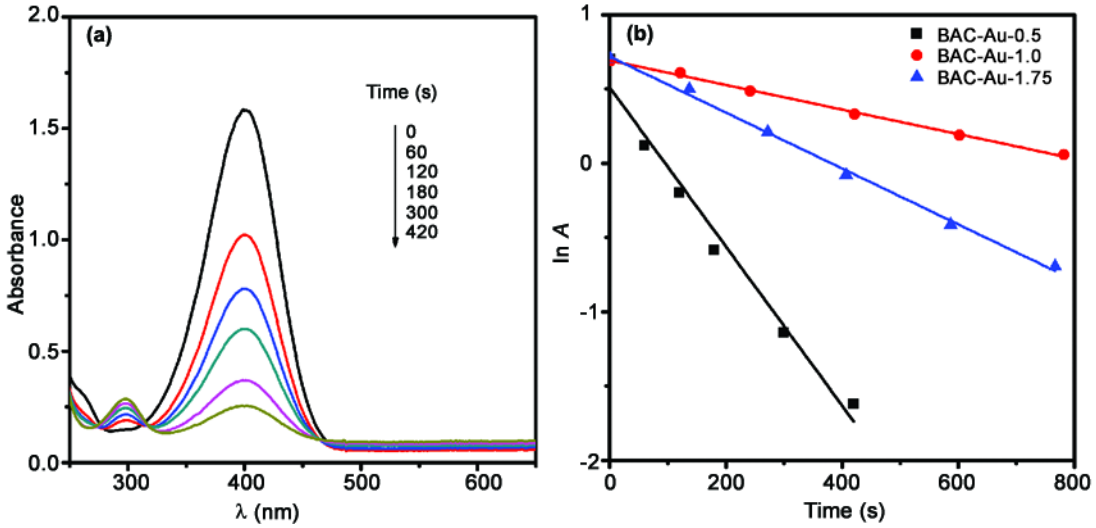

Fig. 7 — (a) Successive UV-vis absorption spectra of the borohydride reduction of *p*-nitrophenol catalyzed BAC-Au-0.5. (b) Plots showing the variation of ln *A* (*A* = absorbance at 400 nm of *p*-nitrophenolate ion) versus time for the reduction of *p*-nitrophenol catalyzed by different samples of network-like Au nanostructures.

that network-like Au nanostructures catalyze the reduction process. In this catalytic reduction process, as the concentration of $NaBH_4$ in the reaction mixture far exceeds the concentration of *p*-nitrophenol, the rate is assumed to follow (pseudo) first order kinetics. Keeping in mind the rate to be first order, we have calculated the values of apparent rate constant (k_{app}) of these catalytic reactions in presence of different network-like Au nanostructures from the linear fitted plot of ln *A* (*A* = absorbance at 400 nm of *p*-nitrophenolate ion) versus time (Fig. 7b). The values of apparent rate constant (k_{app}) for these Au nanostructures are provided in Table 2 that shows that the k_{app} value for sample BAC-Au-0.5 is the highest and is almost 10 times higher in magnitude than that obtained for other samples. However, the k_{app} values of other network Au nanostructures are similar (entry 2 and 3 in Table 2). The differences in the reaction rate might arise due to the smaller sized Au NPs that make the assembled structures.

Redox reactions of $Fe(CN)_6^{3-}$ and $S_2O_3^{2-}$ catalyzed by network-like Au nanostructures

In the case of *p*-nitrophenol reduction, it was observed that the network-like Au nanostructures can effectively catalyze the reaction. Further, to study the response of these network-like Au nanostructures towards inorganic reactions, the redox reaction between $K_3[Fe(CN)_6]$ and $Na_2S_2O_3$ was carried out. This catalytic redox system is easy to perform and the progress of the reaction can be monitored using the UV-vis spectrometer only. Figure 8a shows the decay spectra of $K_3[Fe(CN)_6]$ as its reaction with $Na_2S_2O_3$ is catalyzed by network-like Au nanostructures (sample BAC-Au-1.75). Figure 8a clearly shows the gradual decrease of absorbance of the peak at λ_{max} = 420 nm corresponding to $[Fe(CN)_6]^{3-}$ ions as the reaction proceeded. This indicates that the network-like Au nanostructures could also catalyze the redox reaction of $[Fe(CN)_6]^{3-}$ and $Na_2S_2O_3$. Figure 8b shows the variation of absorbance at 420 nm for $[Fe(CN)_6]^{3-}$ ions with time for the redox reactions catalyzed by network-like Au nanostructures (sample BAC-Au-1.75). The calculated value of apparent rate constant (k_{app}) for this redox reaction is provided in Table 3. The same reaction was carried out using different network-like Au nanostructures and the results are presented in Table 3. The kinetics results reveal that these nanostructures can also be used to catalyze inorganic reactions.

It is known that the catalytic efficiency of a catalyst can be measured from the activation energy. So, to measure the activation energy, we have further carried out the same redox reaction at three different temperatures using same amount of Au nanostructures (sample BAC-Au-1.75). The plots of variation of absorbance with time for these reactions are shown in Fig. 9a. The apparent rate constant (k_{app}) values for these reactions were then used to construct the Arrhenius plot (plot of ln *k* versus 1/*T*) (Fig. 9b) from which the activation energy (E_a) of the redox system was calculated. The activation energy of the reaction catalyzed by network-like Au nanostructures is

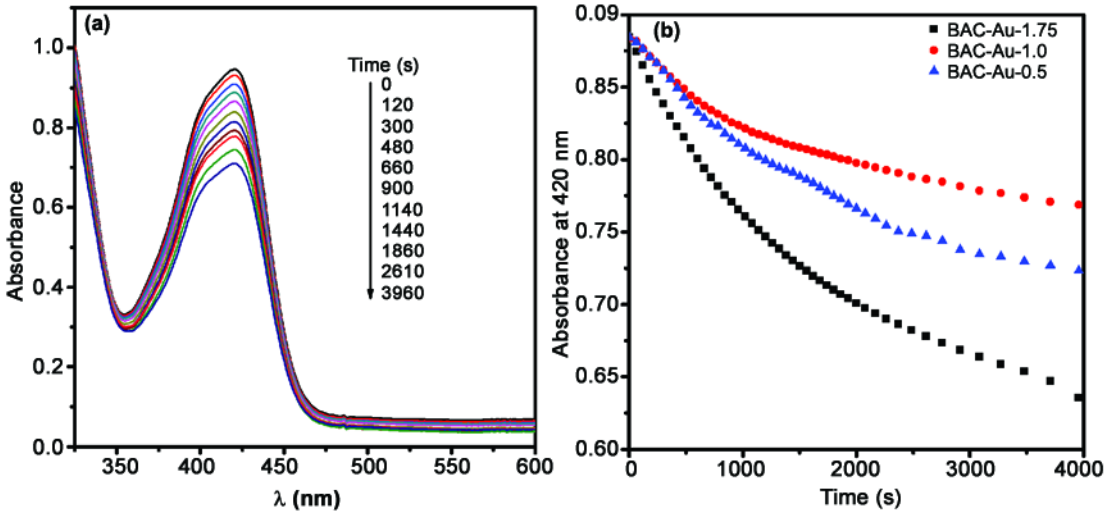

Fig. 8 — (a) Time dependent UV-vis spectra of $K_3[Fe(CN)_6]$ recorded during its redox reaction with $Na_2S_2O_3$ catalyzed by BAC-Au-1.75. (b) Plots showing the variation of absorbance at 420 nm with time for redox reaction between $K_3[Fe(CN)_6]$ and $Na_2S_2O_3$ catalyzed by different samples of network-like Au nanostructures at 25 ºC (Table 3).

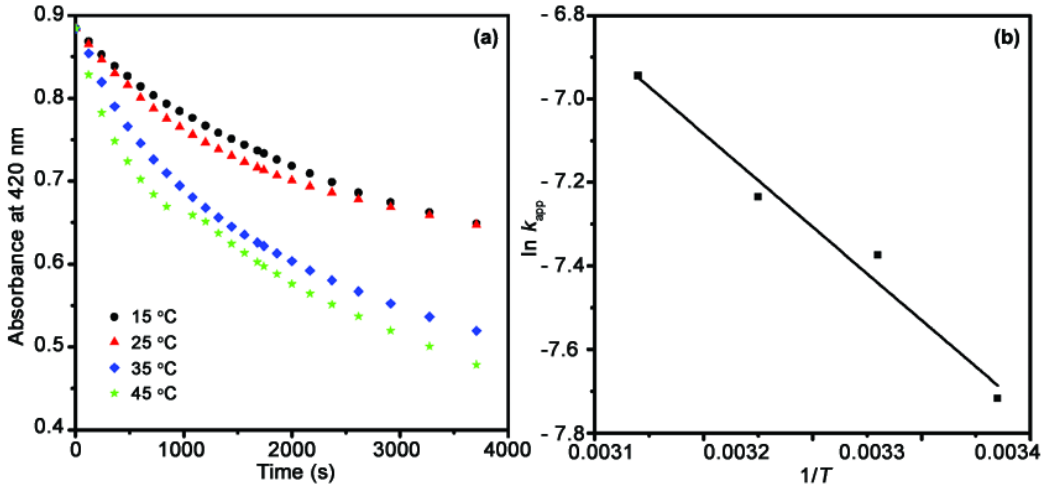

Fig. 9 — (a) Plots showing the variation of absorbance with time for redox reaction between $K_3[Fe(CN)_6]$ and $Na_2S_2O_3$ catalyzed by BAC-Au-1.75 at different temperatures. (b) Plot of ln k_{app} versus $1/T$.

18.7 kJ mol^{-1} which is very low compared to that of uncatalyzed reaction as reported in the literature[42]. Moreover, these values are also comparable to the values obtained for different shaped Pt catalyzed reaction[42].

Reusability of network-like Au nanostructures

It is known that reusability is the main advantage of using heterogeneous catalyst rather than homogeneous catalyst for industrial application. Although a handful of catalytic studies are reported in the literature using Au NPs catalyst, there exist only a few reports where the Au NPs catalyst was recovered for reuse in consecutive cycle of catalysis[21, 27, 28]. Hence, to check the reusability of these network-like Au nanostructures as catalyst in the current system, network-like Au nanostructures (e.g. sample BAC-Au-0.5) were recovered from the reaction mixture after completion of the first cycle of *p*-nitrophenol reduction and used as catalyst for successive batches of catalytic reduction. The data of such reduction reactions are represented by a bar diagram in Fig. 10 that clearly shows that these Au nanostructures are reusable up to seven catalytic cycles. The decrease in the activity may correspond to the weight loss during purification process as also observed in earlier studies[21]. Additionally, a small amount of reactant or its catalysis product may get adsorbed on the surface of Au nanostructures during catalysis by the nascent Au nanostructures[43], which might decrease the activity in the current study.

Similarly, we have also isolated the network-like Au nanostructures catalyst (sample BAC-Au-1.0) from the reaction mixture of $K_3[Fe(CN)_6]$ and $Na_2S_2O_3$ after the first cycle of reaction and the recovered purified Au

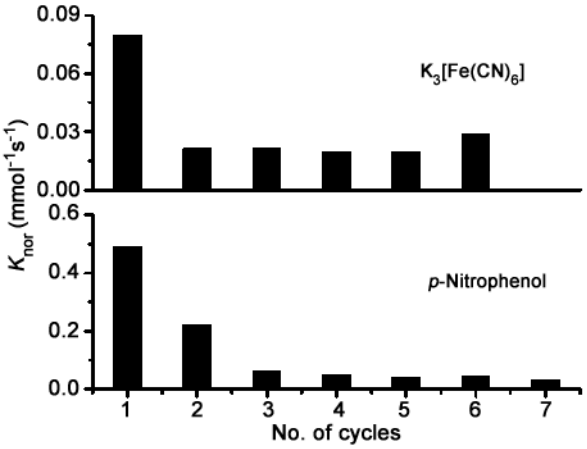

Fig. 10 — The normalized rate constant (k_{nor}) (with respect to the initial amount of catalyst used) in different cycles of catalytic reduction of *p*-nitrophenol and catalytic redox reaction of $K_3[Fe(CN)_6]$ using network-like Au nanostructures. [BAC-Au-0.5 for *p*-nitrophenol reduction, and, BAC-Au-1.0 for redox reaction].

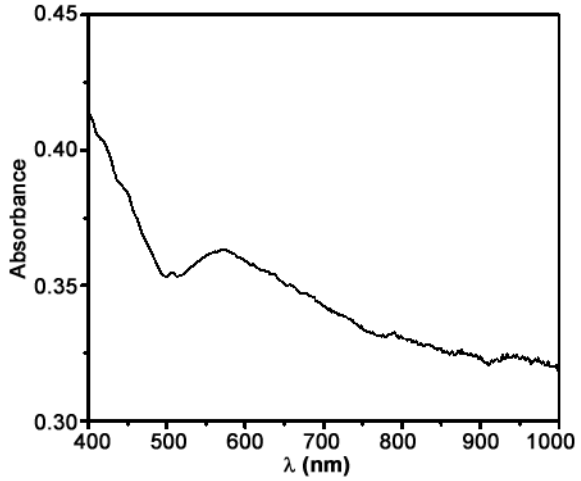

Fig. 11 — UV-vis spectra of the suspension of recovered sample of BAC-Au-1.0 after two cycles of catalytic reaction.

nanostructures were then used as catalyst in a consecutive run of redox reaction between $K_3[Fe(CN)_6]$ and $Na_2S_2O_3$. The results correlating the rate of the reactions normalized with respect to number of moles of the catalyst (k_{nor} values) for such consecutive runs after each cycle are shown in Fig. 10. These results clearly indicate that network-like Au nanostructures are reusable as catalyst up to six cycles in different catalyst systems without much losing its catalytic activity compared to the virgin Au nanostructures. To ascertain the condition of the catalyst after the reaction, the UV-vis spectrum of the recovered BAC-Au-1.0 was recorded after two cycles of catalytic reaction. The spectrum recorded from the suspension of recovered catalyst clearly indicates that the Au nanostructures are stable after catalysis reaction without losing its optical properties which increases the versatility of the catalyst system (Fig. 11).

Conclusions

A novel chemical method to synthesize network-like Au nanostructures by a template-less *in situ* reduction method is reported. In this method, bismuth ammonium citrate was used as reducing agent at room temperature. Microscopic results indicate the formation of different types of network-like Au nanostructures at varying metal ion concentration. Kinetics studies reveal that network-like Au nanostructures are formed by the oriented attachment based self-assembly of spherical nanoparticles and spongy Au nanostructures are probably the intermediates to these network-like nanostructures. These network-like Au nanostructures are catalytically active and can catalyze both organic and inorganic reactions such as borohydride reduction of *p*-nitrophenol and redox reaction between $K_3Fe(CN)_6$ and $Na_2S_2O_3$. Further, these network-like Au nanostructures are reusable up to six cycles without much decay in their catalytic activity.

References

1 Aizpurua J, Hanarp P, Sutherland D S, Käll M, Bryant G W & García de Abajo F J, *Phys Rev Lett*, 90 (2003) 057401.

2 Kelly K L, Coronado E, Zhao L L & Schatz G C, *J Phys Chem B*, 107 (2003) 668.

3 Link S & El-Sayed M A, *J Phys Chem B*, 103 (1999) 8410.

4 Das S K, Parandhaman T, Pentela N, Maidul Islam A K M, Mandal A B & Mukherjee M, *J Phys Chem C*, 118 (2014) 24623.

5 Mandali P K & Chand D K, *Catal Commun*, 31 (2013) 16.

6 Imada Y, Osaki M, Noguchi M, Maeda T, Fujiki M, Kawamorita S, Komiya N & Naota T, *ChemCatChem*, 7 (2015) 99.

7 El-Sayed M A, *Acc Chem Res*, 34 (2001) 257.

8 Niu W, Chua Y A A, Zhang W, Huang H & Lu X, *J Am Chem Soc*, 137 (2015) 10460.

9 Wang L, Guo T, Lu Q, Yan X, Zhong D, Zhang Z, Ni Y, Han Y, Cui D, Li X & Huang L, *ACS Appl Mater Interfaces*, 7 (2015) 359.

10 Sahu S C, Samantara A K, Ghosh A & Jena B K, *Chem Eur J*, 19 (2013) 8220.

11 Scarabelli L, Grzelczak M & Liz-Marzán L M, *Chem Mater*, 25 (2013) 4232.

12 Zhao L, Jiang D, Cai Y, Ji X, Xie R & Yang W, *Nanoscale*, 4 (2012) 5071.

13 Seo D, Park J C & Song H, *J Am Chem Soc*, 128 (2006) 14863.

14 Sun Y & Xia Y, *Science*, 298 (2002) 2176.

15 Chen S, Wang Z L, Ballato J, Foulger S H & Carroll D L, *J Am Chem Soc*, 125 (2003) 16186.

16 Sau T K & Murphy C J, *J Am Chem Soc*, 126 (2004) 8648.

17 Xia Y, Yang P, Sun Y, Wu Y, Mayers B, Gates B, Yin Y, Kim F & Yan H, *Adv Mater*, 15 (2003) 353.

18 Yi S, Sun L, Lenaghan S C, Wang Y, Chong X, Zhang Z & Zhang M, *RSC Advances*, 3 (2013) 10139.

19 Shankar S S, Rai A, Ankamwar B, Singh A, Ahmad A & Sastry M, *Nat Mater*, 3 (2004) 482.

20 Rashid M H, Bhattacharjee R R, Kotal A & Mandal T K, *Langmuir*, 22 (2006) 7141.

21 Rashid M H & Mandal T K, *Adv Funct Mater*, 18 (2008) 2261.

22 Rashid M H, Bhattacharjee R R & Mandal T K, *J Phys Chem C*, 111 (2007) 9684.

23 Bhattacharjee R R, Rashid M H & Mandal T K, *J Nanosci Nanotechnol*, 8 (2008) 3610.

24 Deng J-P, Shih W-C & Mou C-Y, *J Phys Chem C*, 111 (2007) 9723.

25 Schimpf S, Lucas M, Mohr C, Rodemerck U, Brückner A, Radnik J, Hofmeister H & Claus P, *Catal Today*, 72 (2002) 63.

26 Haruta M, Tsubota S, Kobayashi T, Kageyama H, Genet M J & Delmon B, *J Catal*, 144 (1993) 175.

27 Kanaoka S, Yagi N, Fukuyama Y, Aoshima S, Tsunoyama H, Tsukuda T & Sakurai H, *J Am Chem Soc*, 129 (2007) 12060.

28 Miyamura H, Matsubara R, Miyazaki Y & Kobayashi S, *Angew Chem Int Ed*, 46 (2007) 4151.

29 Dauthal P & Mukhopadhya M, *Ind Eng Chem Res*, 51 (2012) 13014.

30 Reddy V, Torati R S, Oh S & Kim C, *Ind Eng Chem Res*, 52 (2013) 556.

31 Sharma N C, Sahi S V, Nath S, Parsons J G, Gardea-Torresde J L & Pal T, *Environ Sci Technol*, 41 (2007) 5137.

32 Narayanan R, *Molecules*, 15 (2010) 2124.

33 Astruc D, Lu F & Aranzaes J R, *Angew Chem Int Ed*, 44 (2005) 7852.

34 Tsunoyama H, Sakurai H, Ichikuni N, Negishi Y & Tsukuda T, *Langmuir*, 20 (2004) 11293.

35 Aiken J D & Finke R G, *J Mol Catal A*, 145 (1999) 1.

36 Narayanan R & El-Sayed M A, *J Am Chem Soc*, 126 (2004) 7194.

37 Rashid M H & Mandal T K, *J Phys Chem C*, 111 (2007) 16750.

38 Tan Y N, Lee J Y & Wang D I C, *J Phys Chem C*, 112 (2008) 5463.
39 Sun L, Song Y, Wei G, Wang L, Guo C, Sun Y & Li Z, *Chem Lett*, 36 (2007) 142.
40 Pong B-K, Elim H I, Chong J-X, Ji W, Trout B L & Lee J-Y, *J Phys Chem C*, 111 (2007) 6281.
41 Chow M K & Zukoski C F, *J Colloid Interf Sci*, 165 (1994) 97.
42 Li Y, Petroski J & El-Sayed M A, *J Phys Chem B*, 104 (2000) 10956.
43 Phukan S, Bharali P, Das A K & Rashid M H, *RSC Adv*, 6 (2016) 49307.